JOURNAL OF PLANKTON RESEARCH | VOLUME 30 | NUMBER 3 | PAGES 333–343 | 2008

The emergence of automated high-frequency flow cytometry: revealing temporal and spatial phytoplankton variability

MELILOTUS THYSSEN[1]*, GLEN A. TARRAN[2], MIKHAIL V. ZUBKOV[3], ROSS J. HOLLAND[3], GÉRALD GRÉGORI[1], PETER H. BURKILL[4] AND MICHEL DENIS[1]

[1]LABORATOIRE DE MICROBIOLOGIE, GÉOCHIMIE ET ECOLOGIE MARINES, CENTRE D'OCÉANOLOGIE DE MARSEILLE, CASE 901, 163 AVENUE DE LUMINY, 13288 MARSEILLE CEDEX 09, FRANCE, [2]PLYMOUTH MARINE LABORATORY, PROSPECT PLACE, THE HOE, PLYMOUTH, DEVON PL1 3DH, UK, [3]NATIONAL OCEANOGRAPHY CENTRE, UNIVERSITY OF SOUTHAMPTON WATERFRONT CAMPUS, EUROPEAN WAY, SOUTHAMPTON SO14 3ZH, UK AND [4]THE SIR ALISTER HARDY FOUNDATION FOR OCEAN SCIENCE, THE LABORATORY, CITADEL HILL, PLYMOUTH PL1 2PB, UK

*CORRESPONDING AUTHOR: melilotus.thyssen@univmed.fr

Received October 29, 2007; accepted in principle January 9, 2008; accepted for publication January 10, 2008; published online January 27, 2008

Corresponding editor: Roger Harris

Phytoplankton observation is the product of a number of trade-offs related to sampling processes, required level of diversity and size spectrum analysis capabilities of the techniques involved. Instruments combining the morphological and high-frequency analysis for phytoplankton cells are now available. This paper presents an application of the automated high-resolution flow cytometer Cytosub as a tool for analysing phytoplanktonic cells in their natural environment. High resolution data from a temporal study in the Bay of Marseille (analysis every 30 min over 1 month) and a spatial study in the Southern Indian Ocean (analysis every 5 min at 10 knots over 5 days) are presented to illustrate the capabilities and limitations of the instrument. Automated high-frequency flow cytometry revealed the spatial and temporal variability of phytoplankton in the size range 1 − ∼50 μm that could not be resolved otherwise. Due to some limitations (instrumental memory, volume analysed per sample), recorded counts could be statistically too low. By combining high-frequency consecutive samples, it is possible to decrease the counting error, following Poisson's law, and to retain the main features of phytoplankton variability. With this technique, the analysis of phytoplankton variability combines adequate sampling frequency and effective monitoring of community changes.

INTRODUCTION

Phytoplankton represents approximately 2% of global photosynthetic biomass, but contributes up to 45% of annual global photosynthesis (Field *et al.*, 1998; Falkowski *et al.*, 2003) and, therefore, is the key to the biologically mediated sequestration of atmospheric CO_2 in the open ocean (Takahashi *et al.*, 1993; Sarmiento and Bender, 1994). To describe the functioning of the biological pump with respect to CO_2 and achieve accurate quantification of its impact on global changes, it is critical to precisely document the spatio-temporal distribution of phytoplankton.

Phytoplankton cells can grow and divide rapidly [up to 2 divisions day^{-1} (Alpine and Cloern, 1988; Furnas, 1991)] and might well react to external variations on an hourly scale. They are metabolically diverse and exhibit a high degree of physiological plasticity (Stewart, 1974; Morris, 1980; Platt, 1981), but they have little buffering capacity to external forcing (Smayda, 1998), which makes them good bio-indicators of their environment and the perturbations to which they are exposed,

doi:10.1093/plankt/fbn005, available online at www.plankt.oxfordjournals.org

providing we know how to extract this information. In addition, phytoplankton is biologically diverse and a large number of species coexist and compete for the same limiting resources (Hutchinson, 1961; Huisman, 1999).

Phytoplankton monitoring techniques have to be able to assess cell abundance at higher frequency than the rate of cell division or mortality (Blanchot, 1997; Vaulot, 1999; Sosik *et al.*, 2003), as well as the rate of environmental changes, which leads to dynamic micro-organism patchiness at scales ranging from a few centimetres to hundreds of kilometres (Cassie, 1963; Young *et al.*, 2001; Mitchell *et al.*, 2005; Martin *et al.*, 2005). Consequently, our present knowledge is limited by the frequency with which phytoplankton can be sampled and analysed. This limitation is due in part to the microscopic size of the cells, their high morphological heterogeneity and to the simple fact that they live in a dynamic environment which remains difficult to reach, particularly away from the coasts.

Current phytoplankton observations are, by default, simplified. Optical microscopy documents the taxonomic diversity of phytoplankton, but is time-consuming and therefore cannot be employed for spatial or temporal surveys of high resolution. Conventional flow cytometry analyses single cells at a high rate (up to several thousands cells per second) and thus enables significant progress in addressing the spatio-temporal distribution of phytoplankton, particularly the smallest cells ($<10-20$ μm in size) (Burkill, 1987; Li, 1997). However, this single-cell analysis does not account for larger cells or chains that are rarely concentrated enough for conventional flow cytometers (Zubkov and Burkill, 2006). Pigment analysis provides some complementary information about the phytoplankton assemblages in many ecosystems but does not resolve fine temporal scales (Ston *et al.*, 2002) and it provides only index estimates of phytoplankton group abundance or biomass. Fluorometry allows a good spatio-temporal coverage of chlorophyll *a* concentrations (Rantajarvi *et al.*, 1998), but does not provide any information on phytoplankton assemblage composition. Remote sensing (satellites) generate a synoptic view of sea surface phytoplankton distribution that is out of reach of field measurements (ships for instance), but the low spatial resolution of this technique means that it is limited, particularly in heterogeneous coastal areas where phytoplankton is usually at its most abundant and highly dynamic. Remote sensing also does not account for short-time (hourly) scale variations.

Flow microscopy has been further developed to enumerate morphologically identifiable, usually larger (>20 μm) phytoplankton cells (Sieracki *et al.*, 1998) by coupling flow cytometry with image analysis of counted micro-organisms. Being image based and designed to analyse larger cells (generally >50 μm), the optical resolution of the cameras and objectives are not well suited for analysing smaller particles, so that cells, particularly <20 μm in size are not readily resolved.

Flow cytometry is a powerful technology to investigate micro-organisms. New instruments were designed to cover the full-size range of phytoplankton ($\sim$1 up to several 100 μm) and be operated *in situ*. The FlowCytoBot (Olson *et al.*, 2003; Sosik *et al.*, 2003) was for the first time successfully deployed on a monthly basis and observations were limited to pico- and nano-phytoplankton as conventional instruments. A new generation of the FlowCytoBot is coupled to an image in-flow system to cover the size range 10 to $\sim$100 μm (Olson and Sosik, 2007), with an improvement in automated image analysis (Sosik and Olson, 2007).

The other emerging technique for *in situ* high-frequency monitoring of phytoplankton (analysis frequency up to one sample every 5 min) is a new generation of flow cytometer (Cytobuoy, Dubelaar *et al.*, 1999; Dubelaar and Jonker, 2000), fully automated and delivering real-time data when operated on-line. Phytoplankton resolution by this instrument is based on the pulse-shape analysis and to our knowledge, it is the only one to do so. In the present study, we examined the efficacy of the Cytobuoy flow cytometry for resolving fine temporal and spatial phytoplankton distributions in coastal and oceanic surface waters. This was achieved by using comparisons with conventional flow cytometers and by running inter-calibration exercises between two Cytosubs. We also report on the performances of the instrument when monitoring phytoplankton at high-frequency (30 min) at a fixed point and when using it for determining phytoplankton surface distribution along a ship's track by sampling every 5 min. Advantages and limitations of the instruments used are discussed.

METHOD

Flow cytometers

Two Cytosub flow cytometers (Cytobuoy b.v., Netherlands) were used in the present study. One instrument is based at the Laboratoire de Microbiologie, Géochimie et Ecologie Marines, Marseille, France (LMGEM). The other instrument is based at the National Oceanography Centre, Southampton, UK (NOCS). The specifications of the NOCS Cytosub and the LMGEM instruments are similar except that the power source of the former is a lithium battery (24 V

DC) encapsulated in an external cylindrical pressure housing. The LMGEM Cytosub was connected via cable for energy supply and real-time data transfer to a computer. In addition, the data generated by the NOCS instruments was saved on a data logger, from which it was transmitted to a computer using a BlueTooth connection. According to their specifications, the Cytosub instruments can analyse large phytoplanktonic cells (1 to ~800 μm in width and a few mm in length) and relatively large water volumes (up to 4 cm^3 per sample). Instruments can be operated online or as a submersible instrument, down to 200 m depth, being protected by a cylindrical aluminium pressure housing. Sample water is pumped to fill a sample loop of 4 cm^3 before entering the flow cell in order to avoid external turbulences and to enable operation at atmospheric pressure. The minimum sampling interval is 5 min, which includes flushing of the sample loop, sample analysis and data transfer.

The sample flow rate of the LMGEM Cytosub was 7.8 $mm^3\,s^{-1}$ during the field survey and 8.3 $mm^3\,s^{-1}$ during the inter-calibration experiment with the NOCS Cytosub due to differences in diameters of sample tubing used. The sample flow rate of the NOCS instrument was 11 $mm^3\,s^{-1}$. The instruments used 0.2 μm filtered seawater containing ~1% paraformaldehyde fixative as a sheath fluid. The sheath flow rate was 4800 $mm^3\,s^{-1}$. The sheath fluid and the analysed seawater were mixed together at the output of the flow cell and filtered through a 0.2 μm Polycap ™ AS Nuclepore cartridge in order to be recycled. Each particle was intercepted by a laser beam (Coherent solid-state Sapphire, 488 nm, 15 mW). The light scattered at 90° (side scatter, SWS) and fluorescence signals were dispersed by a concave holographic grating and collected via a hybrid photomultiplier. The forward scatter (FWS) signal was collected via a PIN photodiode. The red (FLR), orange (FLO) and yellow (FLY) fluorescences were collected in the wavelength ranges 668–734, 601–668 and 536–601 nm respectively. Data recording was triggered by the FWS signal. The shape of the signals was encoded with a 4 MHz frequency and data were saved in distinct 64 kb grabbers. Particles traversed the 5 μm laser beam at a rate of 2 m s^{-1}. This meant that the FWS signal shape of 1 μm beads would be defined by ~12 points. More generally, particles flowing along their long axis (L (μm)), would have the shape of their FWS signal defined by:

$$\text{Number of data points defining FWS shape} = 2 * (5 + L) \quad (1)$$

Two conventional flow cytometers were used to calibrate the Cytosub. (i) A Cytoron (Cytoron Absolute, ORTHO Diagnostic Systems), equipped with an air-cooled 488 nm argon laser. The sample and sheath rates were 1 and 100 $mm^3\,s^{-1}$, respectively. (ii) A MoFlo (Dako), equipped with a dual line, water cooled, Coherent laser (351 and 488 nm). The MoFlo flow rate was determined by weighing the sample before and after 3 min of sample analysis.

Software

Cytoclus software (version 2004, Cytobuoy b.v.) was used to analyse the data collected by the Cytosubs. Clusters were selected by taking into account the amplitude and the shape of the different signals. In addition to five average signal heights for FWS, SWS and for three fluorescence signals: FLR, FLO and FLY, some simple mathematical models were assigned to each signal shape: inertia, fill factor, asymmetry, number of peaks, length, apparent size (FWS size) (Dubelaar *et al.*, 2003). All these values are summarized in cytograms that facilitate the identification of clusters of cells with similar optical properties derived from those mathematical models.

Data from the MoFlo (FCS files) were analysed using Summit© software (Dako) and those from the Cytoron with Immunocount© (Ortho Diagnostic Systems).

Culture analysis

Four phytoplankton species *(Dicrateria inornata, Prymnesium patelliferum, Pleurochrysis carterae, Pleurosigma trigosum)* from the Plymouth Culture Collection were grown on F/2 medium (Guillard, 1975). Cells were diluted in 0.2 μm filtered seawater for comparative analyses with both Cytosub instruments.

Bead analysis

Several fluorescent microspheres from Beckman Coulter [Flow-Set™ fluorospheres (3.6 μm) Flowcount™ fluorospheres (10 μm)], and Polysciences Fluoresbrite fluorospheres (2 μm, 3 μm) were used to test the instruments. Each sample was manually and gently homogenized to prevent electrostatic adhesion between beads and adsorption on the tube wall (Brando *et al.*, 2001).

Counting reproducibility

Reproducibility of flow cytometric counting was determined using 10 and 3 μm beads at a range of bead concentrations. Each bead sample, manually

homogenized, was analysed 5–15 times with the LMGEM Cytosub. The coefficient of variance of the Cytosub counts (CV_c) was derived from the arithmetic mean of the counts ($\bar{u}$) and their standard deviation (SD):

$$CV_c = \frac{100 * \mathrm{SD}}{\bar{u}} \quad (2)$$

The variability of a measured particle concentration is the sum of the instrument variability and the population variability. The counting of rare particles is significantly affected by Poisson's law (Gosset, 1907; Kirchman, 1982; Shapiro, 2003). The variability of counting rare particles is due to the number of particles counted by the instrument which depends on the volume analysed per unit of time. Following Poisson's law, for any count the theoretical coefficient of variance is:

$$CV_p = \frac{100}{\sqrt{n}} \quad (3)$$

n being the number of counted particles.

Field inter-calibration of Cytosubs

Both Cytosubs were installed on a small boat and were powered by a portable generator. Twelve stations were occupied at 30 min intervals along a South–North transect in the Bay of Marseille (Fig. 1A). Surface seawater was collected at each station with a bucket and directly analysed by both Cytosubs.

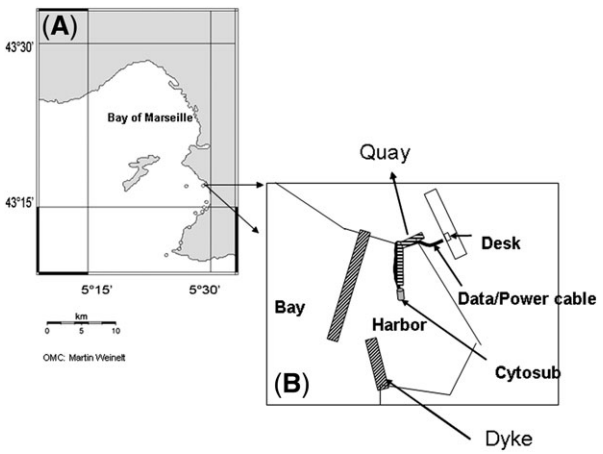

Fig. 1. (**A**) Sampling area in the Bay of Marseille, France. The open dots correspond to the sampling sites for the NOCS and LMGEM Cytosub inter-calibration experiment. (**B**) Detail of the sampling harbour in the Bay of Marseille where the high-frequency time series was run with the LMGEM Cytosub that was fixed at the end of a quay and directly connected to a computer via a waterproof data/power cable.

Field investigations

Time series

Phytoplankton abundance was monitored at a fixed site in a semi-enclosed harbour in the Bay of Marseille (43°17′N, 5°22′E, France, Fig. 1) during summer 2005 at a frequency of one sample every 30 min. The LMGEM Cytosub was fixed at the end of a jetty at a depth of 1.5 m and connected via a waterproof cable to a main electricity supply and a computer (Fig. 1B).

Online spatial coverage

An autonomous underway sampling regime was carried out using the NOCS Cytosub on board the Royal Research Ship Discovery during cruise (D285) to the Crozet Islands in the Southern Indian Ocean in November–December 2004 (Fig. 2). Samples were analysed from the ship's non-toxic continuous seawater supply, drawn from a depth of 5 m. A 5 min or 1.5 km sampling interval was maintained over a period of 5 days.

Data treatment

According to Poisson's law, the number of counted cells in a selected cluster in a natural sample can be too low to reach a coefficient of variance (CV) <3%. In order to reduce the CV and compare the cluster dynamics

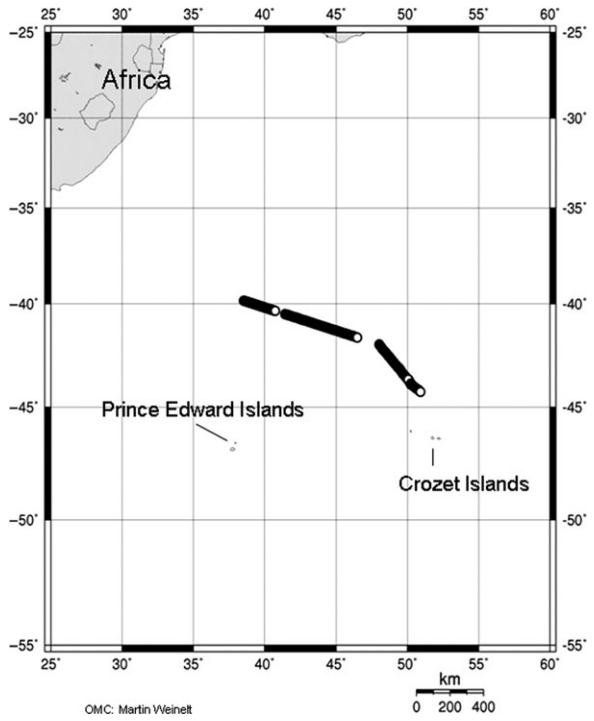

Fig. 2. Study area of the D285 cruise onboard the RRS Discovery.

from single analysed samples that may be undercounted, a set of samples was combined, increasing the number of counted particles in the selected cluster. The cell concentration calculated from counts in a cluster at a single sample level was then compared with the cell concentration calculated by adding successive counts from the same cluster in a set of samples. The number of combined samples integrate 3 h sampling in the case of the temporal study (6 combined samples), and 7.5 km in the case of the spatial study (5 combined samples). The different integration steps show the trade-off between the increasing significance in counting and the decrease in the high resolution of the initial signal. As an example, for any given cluster C in a given sample S_k ($k = 1$ to r), the total particle count within C is n_k.

The sum P of counted particles falling within C over the r samples is:

$$P = \sum n_k (k = 1 \text{ to } r) \tag{4}$$

The overall analysed volume V is

$$V = \sum v_k (k = 1 \text{ to } r) \tag{5}$$

where v_k is the analysed volume in sample k.

The CV as calculated in equation (2) (CV_P) for the particles summed up in the cluster C for r samples is:

$$CV_{PC} = \frac{100}{\sqrt{P}} \tag{6}$$

The cell concentration derived from combined counts in the cluster C for r samples is obtained by dividing the sum of counted particles with the sum of analysed volumes (P/V).

The data were then compared to a sampling frequency of 12 h and 15 km for both temporal and spatial experiments, respectively.

RESULTS

Size validation and comparison with conventional flow cytometers

Concentrations of fluorescent beads of various diameters were determined using the LMGEM Cytosub and conventional flow cytometers. When assessing the counting accuracy of the Cytosub, we compared the absolute counts of the same bead samples, obtained with the Cytosub, the Moflo and the Cytoron. They were similar within experimental uncertainties ($y = (0.78 \pm 0.04)\,x + (11\,129 \pm 7849)$, $r = 0.99$, $P < 0.001$; $y = (0.97 \pm 0.11)\,x + (4351 \pm 17\,082)$, $r = 0.95$, $P < 0.001$ for the Moflo and the Cytoron, respectively) as illustrated by Fig. 3.

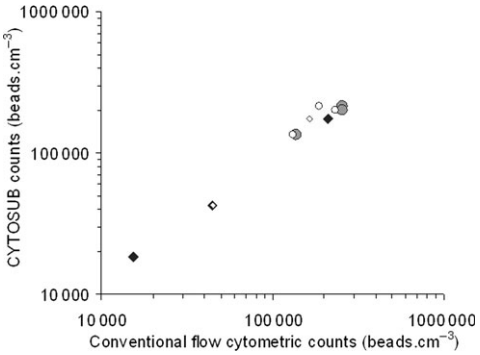

Fig. 3. Inter-comparison between the Cytosub and conventional flow cytometers (Moflo and Cytoron). Filled symbols: comparison between the Cytosub and the Moflo. Open symbols: comparison between the Cytosub and the Cytoron. Diamond: 3.6 μm beads, circle: 10 μm beads.

To determine the accuracy of the size estimation derived from the shape of particle FWS, the average number of data points for 10 and 3 μm beads analysed with the Cytosub (Fig. 4A) was compared with the theoretical data point number calculated from formula (1). Results reported in Table I show a good match between experimental and theoretical values.

In Fig. 4B, counts from the reproducibility experiment were plotted against the standard deviations using both relationships: CV_c [equation (2)] and CV_p [equation (3)]. For instance, when $>10^3$ particles were counted, the reproducibility was achieved with a $CV < 3\%$ and both standard deviation calculations had similar trends.

Cytosub inter-calibration

Cytograms in Fig. 5A show the two main clusters ($C1$ and $C2$) that were used for the inter-calibration experiment involving natural samples collected in the Bay of Marseille. Differences observed on the upper and lower cytograms are due to the threshold set for recording FLR (15 for the LMGEM Cytosub and 20 for the NOCS Cytosub, on a scale of 0–256). The $C1$ and $C2$ cluster concentrations ranged between approximately 750 and 8000 cells cm^{-3} and culture concentrations (clusters not shown) varied between approximately 2000 and 110000 cells cm^{-3}. The CV_P [equation (3)] characterizing counts within $C1$ were between 3.5 and 5.5%. They varied between 2 and 5% for counts within $C2$. The $CV_p < 2\%$ was predicted for the counts of the

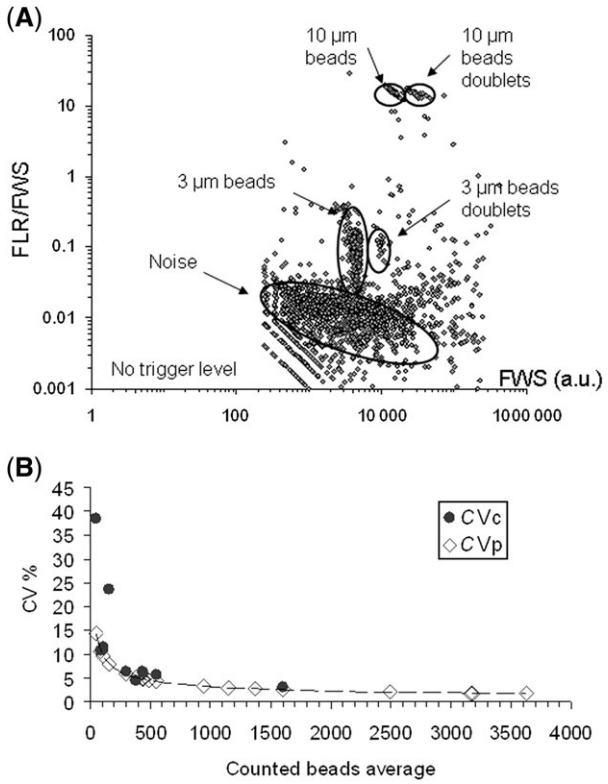

Fig. 4. (**A**) CytoClus cytogram of 3 and 10 µm beads and their doublets during the reproducibility test. FWS and FLR values are derived from the cell red fluorescence and FWS shape signal amplitudes of each particle. The FLR/FWS is the ratio of the corresponding pulse shape signals. It is used because the difference between FLR and FWS pulsed shape signals is most of the time very weak and the use of the ratio helps to differentiate them. (**B**) Comparison between experimental repeated Cytosub bead counts (n) versus their calculated coefficient of variance and artificial counts (n) versus their theoretical Poisson's coefficient of variance ($100/\sqrt{n}$), see formula (3). Black circles: average repeated counts of beads ($\bar{u}$, samples were counted between 5 and 15 times) versus the corresponding coefficient of variance ($CV_C = (100*SD)/\bar{u}$). White diamonds: artificial counts (n) versus their theoretical Poisson's coefficient of variance ($CV_P = 100/\sqrt{n}$).

Table I: Commercial beads of 10 and 3 µm analysed with the Cytosub in order to compare the theoretical and experimental number of data points, dependent on the bead size, the laser beam width, the laminar flow rate and the analog to digital converter

Bead size (µm)	Average calculated length (µm)	Average number of data points for FWS shape	Expected number of data points 2 * (*L*+5)
10	9.9 ± 0.3 (n = 98)	29.3 ± 1.2	30
3	2.8 ± 0.4 (n = 653)	17.2 ± 0.8	16

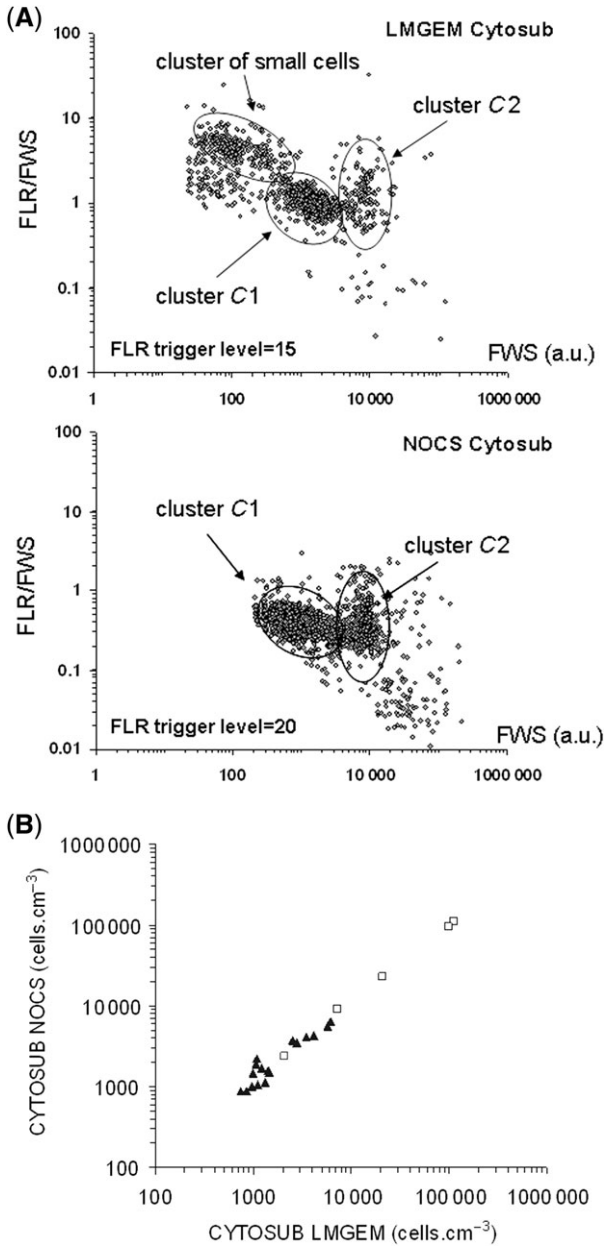

Fig. 5. (**A**) Cytograms (as described in Fig. 4A) of natural seawater and selected clusters observed with the LMGEM Cytosub (upper cytogram) and the NOCS Cytosub during the inter-comparison sampling in the Bay of Marseille. Two main clusters were compared, *C*1 and *C*2. Note that small cells were present on the LMGEM cytogram because of a lower threshold on the FLR (level = 15 (range = 0–256)) than for NOCS analysis (level = 20). (**B**) Result of the inter-comparison between the NOCS Cytosub and the LMGEM Cytosub. Black triangles: abundance comparison of *C*1 and *C*2 clusters (cells cm^{-3}) from natural samples (Fig. 5A). White squares: abundance comparison of different phytoplankton cultures (cells cm^{-3}; see text for details). Note that the graph is on a log scale.

phytoplankton cultures of high cell density. A relationship was observed between parallel counts made on the NOCS and LMGEM Cytosubs (Fig. 5B) of phytoplankton cultures and natural seawater samples (*C*1 and *C*2, Fig. 5A) with a statistically significant correlation coefficient of $r = 0.99$, $P < 0.001$.

Field investigations

Time series

Figure 6A shows cluster $C1_M$ resolved during the summer 2005 time series and its time course by the end of July with the corresponding theoretical standard deviation per sample using Poisson's law (Fig. 6Ba). The data in Fig. 6Ba provide evidence for diel variations and a slow increase in cell abundance occurring at a longer time scale. Cluster $C1_M$ is one of the groups made by the smallest cells resolved by the instrument and was observed during the whole sampling period (average estimated length was 1.6 ± 0.34 μm and average FWS size estimation was 1.5 ± 0.3 μm). The average count for $C1_M$ was 440 ± 179 cells per sample during July 2005, which corresponds to an average CV_P [equation (3)] of 4.7%, varying between 3.3 and 11.3% (Fig. 6Ba). The relatively low value of the count is partially due to a set of non-target events (noise and air bubbles) filling the memory before sufficient volume was analysed. Clusters other than $C1_M$ are visible on Fig. 6A, with higher FWS and FLR values. However, their accurate counting required the use of a higher threshold on fluorescence or scatter parameters to remove the noise and smaller cells. Under these conditions, a total of five other clusters were defined (data not shown) during the whole sampling period. Counts varied from 1 to a few hundreds of cells per cluster continuously observed over more than 436 samples analysed during July 2005.

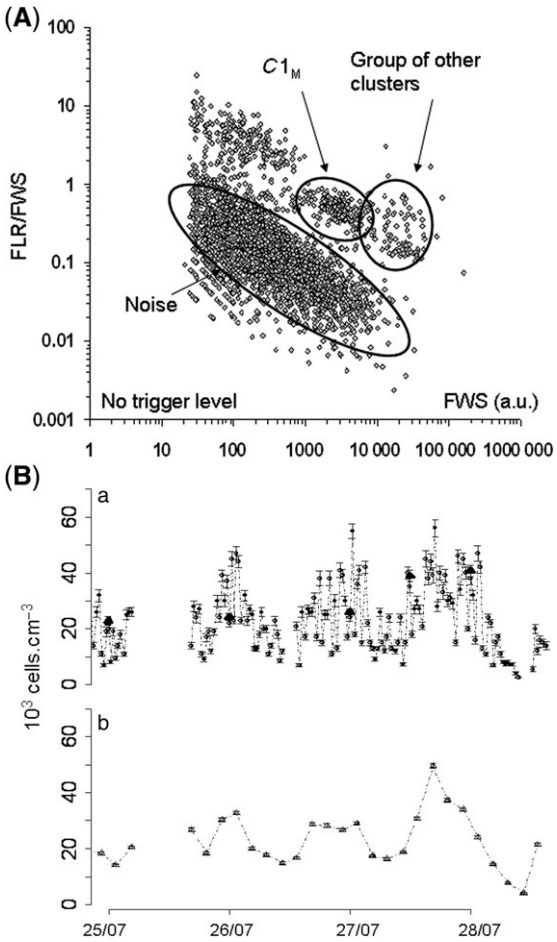

Fig. 6. (**A**) Cytogram (as described in Fig. 4A) of natural seawater analysed during the July 2005 temporal study in a harbour of the Bay of Marseille (Fig. 1B) and the selected cluster $C1_M$. (**Ba**) Circles: distribution of $C1_M$ abundance (10^3 cells.cm^{-3}) sampled every 30 min with the corresponding standard deviation calculated from the theoretical Poisson's law CV_P [see text, formula (3)]. Black triangles: selection of 12 h spaced samples. (**b**) Circles: integration of six samples by combining the counts of $C1_M$ cluster divided by the total volume analysed during those six samplings with the corresponding standard deviation calculated from the theoretical Poisson's law CV_{PC} [see text, formula (6)].

Regarding $C1_M$, adding consecutive counts over 3 h (six samples) yielded a CV_{PC} [equation (6)] of ~3.4% on average but still demonstrates a well defined diel cycle (Fig. 6Bb). Sampling over a larger period (12 h, black triangles in Fig. 6Ba) may still reflect the trend of abundance variations but not that of the diel cycles.

Spatial distribution

Figure 7A shows the cluster $C1_c$ selected to illustrate its spatial variation during the D285 cruise. Figure 7Ba illustrates its abundance distribution with the corresponding theoretical standard deviation per sample, CV_P [equation (3)]. Spatial data were retrieved with the same method as temporal data. The average count for $C1_c$ was 284 ± 159 cells, which corresponds to an average CV_P [equation (3)] of 5.9%, varying between 3.8 and 12.8% (data not shown). The relatively low counts per sample were again partially due to a set of non-target events (noise and air bubbles) filling the data grabbers before sufficient volume was analysed.

As for the time series data, summing counts of five samples (equivalent to 7.5 km of cruise track; Fig. 7Bb) gave a good estimation of the overall trend with CV_{PC} [equation (6)] of <2.4%. Black triangles in Fig. 7Ba show the effect of selecting samples at a frequency of 15 km with the corresponding theoretical standard deviation CV_P [equation (3)].

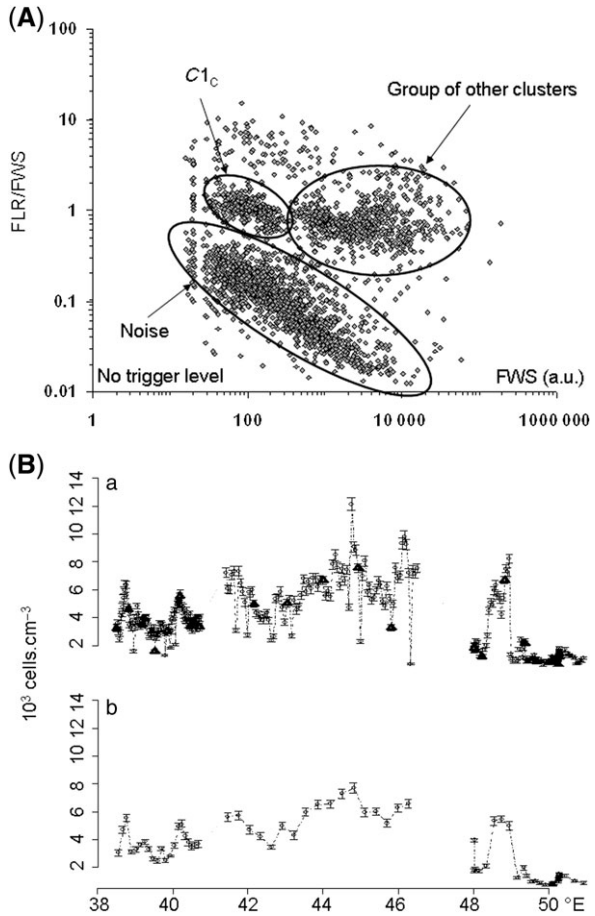

Fig. 7. (**A**) Cytogram (as described in Fig. 4A) of natural seawater analysed during the spatial study in November–December 2004 (Fig. 2) and the selected cluster $C1_C$. (**Ba**) Distribution of $C1_C$ abundance (10^3 cells cm^{-3}) derived from sampling every 5 min with the corresponding standard deviation calculated from the theoretical Poisson's law CV_P [see text, formula (3)]. Black triangles: selection of 15 km spaced samples. (**b**) circles: integration of five samples by combining the counts of $C1_C$ divided by the total volume analysed during those five samplings with the corresponding standard deviation calculated from the theoretical Poisson's law CV_{pc} [see text, formula (6)].

DISCUSSION

Comparison of particle enumeration by Cytosub and conventional flow cytometers

Cytosub counts were highly correlated with those of conventional flow cytometers (Fig. 3). Results illustrated in Fig. 4B demonstrate that the count accuracy is determined by the Poisson's probability distribution, which is only dependent on the flow rate of the sample in the instrument and on the memory size of the data grabbers. The deviation observed between the Cytosub counts CV_C [equation (2)] and the Poisson's theoretical CV_P (3) (Fig. 4B) estimates the instrument variability, which does not exceed 3% (G. Dubelaar, Netherlands, personnal communication). Using the Cytosub in its present configuration, counting accuracy of a selected cluster depends on the recording time which in turn depends on the concentration of the particles and on their size. Consequently, a sample of large particles will lead to a shorter recording time than a sample with small particles of similar concentration.

The count accuracy could be easily improved by increasing the memory size in order to collect more particles per sample. In natural samples, the upper limit of the size range analysed is defined by the cell concentration and consequently the volume analysed. The new version of the automated instruments from the Cytobuoy company are no longer limited in data recording, both in terms of disk space and data transfer rate as the instruments are now equipped with Universal Serial Bus (USB) data transfer coupled with high content buffers. With this new configuration, the size range of analysed phytoplankton will be highly expanded but the analysis of the largest cells will face the same counting limitations. The inter-calibration exercise demonstrated a strong correlation between parallel measurements conducted both with phytoplankton cultures and natural samples (Fig. 5B).

The size estimations conducted with the set of beads used during the inter-calibration experiments (Table I) substantiated the accuracy of the size definition for cells in their natural environment. As with any instruments, frequent calibrations should be conducted since it is not possible to add beads to seawater samples during the *in situ* analysis. In a normal situation, the average cell size within the main clusters should not be subject to change more than one would expect within a normal cell cycle. Consequently, a strong variation in the FWS pulse shape within all clusters during high-frequency sampling should be taken as a warning signal for laser beam displacement or flow rate change in the flow cell. Thus, the above results help validate comparisons between laboratory and field studies conducted with different Cytosubs.

Examples of high-frequency phytoplankton analysis

Time series

High-frequency phytoplankton monitoring is critical to define the time of day and frequency at which other measurements should be conducted to best characterize the phytoplankton assemblage and its environment. Automated phytoplankton analyses at a frequency of one sample every 30 min over a few weeks have never been previously undertaken. The automated high-frequency

analysis of phytoplankton at a fixed site demonstrated the capacity of the Cytosub to account both for diel variations and larger time-scale trends (Fig. 6B).

In the reported example, it is shown that the high-frequency sampling can be used to compensate for the limitations in absolute counts imposed by the instrument memory capacity. Indeed, by combining successive counts, the count accuracy is improved and evidence for diel variations and longer term trends remains (Fig. 6Bb). Knowledge of diel cycles through cell abundance variation, combined with optical parameter data measured over several weeks allow the calculation of growth rates in order to define the level of synchronicity in the cell cycles (Campell and Yentsch, 1989). Once the dynamics of the different clusters is known, it becomes easier to define external factors acting on the behaviour of those clusters at the cell cycle level. At present, the reported time series demonstrates that analysing one sample every 3 h in the Bay of Marseille, despite some uncertainty in the counting, is sufficient (Nyquist, 1928) to account for the natural variability in cell abundance due to the impact of physiological behaviour (cell migration, cellular division) and external forces (wind impact, advection).

Sampling at a lower frequency is only accurate if the instrument is able to collect enough cells per single sample and if the cluster cycles are known, even if some decrease in cell abundance over a few days may be due to a slow down of the growth rate (Sosik *et al.*, 2003). But, as illustrated on top of the real sampling frequency (Fig. 6Ba), sampling at a frequency of 12 h (black triangles) suppresses the evidenced diel cycle and makes it difficult to discriminate between external factors and physiological cycles when interpreting the cell abundance variations.

In addition to diel cycles, significant variability (Fig. 6Ba) in cell abundance within a given cluster was observed between samples (every 30 min). As with the $C1_M$ during July 2005, the variability between successive samples reached 57% in 25% of the cases. Recorded variations can be generated by a low count within a cluster (up to $\sim$11%), or by instrument variability (up to 3%). Errors are cumulative, so that each sample may be affected by a maximum of 15% variability, which is insufficient to explain the observed variability. This natural short-term variability may be explained by patchiness (Doubell *et al.*, 2006), water mass displacement, external factors (tides, grazing, weather events) and behavioural factors (motility, vertical migration).

Spatial coverage

Compared to high resolution temporal sampling, spatial sampling at a high resolution reveals both cell cycle variability and patchiness of cell abundance (Fig. 7Ba). High spatial resolution sampling improves the ability to define phytoplankton patches. Decreasing the spatial resolution by combining data from successive samples does not always lose the trend of spatial distribution (Fig. 7Bb). The variability between samples at a high spatial resolution may combine the biological variability that could increase the patchiness signature and decrease the evidence of physical impact. This analysis allows the establishment of the trade-off that is needed in order to link phytoplankton distribution and physical forcing at a sub meso-scale (1–10 km) level. There is, however, evidence that biological and physical fields do not match and it is impossible to explain spatial cell distribution only from physical forcing (Zubkov *et al.*, 2002; Martin *et al.*, 2005).

It is clear that combining accurate spatial and temporal sampling is crucial to estimate global phytoplankton biomass. Theoretically, in order to best define patchiness in open waters, the sampling procedure must operate at a temporal scale that includes intrinsic variability such as cell cycle or predation, and at a spatial scale that fits the involved hydrological features, in terms of coverage and dynamics. Phytoplankton cell cycle should not vary drastically from one place to the other, since it is essentially driven by the light-dark cycle. However, more variability can be expected from spatial features and mixing processes. The Cytosub automated analysis capacities will meet these requirements, in particular for sub meso-scale features such as eddies and fronts, including the hour scale biological processes as patchiness factors.

Advantages of the instrument

The current configuration of the Cytosubs enables effective analysis of phytoplankton in a size range between approximately 1 to 50 μm, with little statistical significance for larger cell observations. Significant counts of larger cells are possible using cultures or maybe during highly concentrated blooms. The new Cytosub version benefits from high rate data transfer and large storage capacities which expand the size range of phytoplankton cells that can be significantly analysed. However, cells close to the upper limit will face the same statistical limitation due to their lower concentration. Automation of sampling and analysing *in situ* or using pumped water enables the analysis of phytoplankton at high resolution. Economic advantages are important since automation implies reduced workforce involvement and capacity to sample remote areas without a constant need to visit the sampled site. Analysing one sample every 10 min is very cost effective. Many advantages of the instrument stem from its flexibility of deployment (high-frequency sampling or

in situ sampling), the ability to programme the instrument for automatic analysis of samples, and the multiparametric measurement of particles. Shape/pulse recording enables a greater definition of selected cells in regards to physiological and morphological diversity. Even if many of the pico- and nanoplankton cells are broadly oblate spheroids and morphologically homogeneous, the Cytobuoy flow cytometer increases the potential for discrimination between larger cells (20–50 μm) where morphology aids more in discrimination. Sampling at such a high temporal frequency combined with information on individual cells is of great importance in the observation of phytoplankton dynamics. This higher frequency is a solution to the under-sampling that persists for large and dispersed cells, because the presence of those cells over a few hundreds of samples covering a few tens of days is valuable qualitative information which would not be considered if sample frequency was low. The ataxonomic selection of cells based on their optical properties offers a simplified view of phytoplankton diversity based on morphological criteria. Those criteria may afford information on the status of the environment since cell physiology and morphology are tightly coupled to the status of the surrounding environment.

Scientific advantages will increase with high resolution observations. Vertical locomotion behaviour, bio-indicators of water mass changes or of local pollution events and *in situ* cell cycle observation are examples of domains that may be investigated.

Limitations of the instrument

The Cytosubs deployed in this study only analysed between 1500 and 2500 particles per sample in natural seawater. This is primarily because of hardware memory constraints (64 kb data grabbers for each parameter acquired) but even after reducing this limitation, many groups of micro-organisms in their natural environment will remain under-sampled because of their low concentration that may occur at any stage of their development. High-frequency sampling will thus appear as an additional process that will minimize errors from undercounting. Because the instrument triggers acquisition on FWS in order to obtain time resolved pulse-shape analysis of particles, the background may look highly noisy due to lots of non-fluorescent particles that occupy a large proportion of available memory. Similarly, large cells also require a large memory space. This constraint means that presently the analysis of large cells is mostly qualitative rather than quantitative.

It has been found that, for natural samples it is not normally possible to quantify particles larger than ~50 μm in size on abundance grounds, although the instrument is designed to analyse cells over more than 1000 μm in length. Even if a large number of clusters can be resolved in natural samples, the abundance of any single cluster may be too low to be statistically significant for abundance estimation. The solution is to combine counts of several clusters. This has the effect of providing statistically significant counts at the expense of decreasing the effective sample frequency/spatial coverage when conducting temporal/spatial studies under a particular set of conditions. However, since the instrument is able to run automated high-frequency analysis, the principal information on dynamics and abundances of what is observable is maintained.

The Cytosub instrument is a powerful tool providing access to simple automated analysis of phytoplankton assemblages ranging from 1 up to 50 μm in natural samples. It is now possible to study phytoplankton communities in space and time with information on their optical and dimensional diversity more effectively than a decade ago. Some technical improvements such as an increase in the volume analysed per unit of time and the already effective increase in memory capacity and data transfer should give the access to the distribution in natural samples of phytoplankton cells ranging from one to hundreds of micrometres.

However, at present, in order to carry out a complete analysis of phytoplankton communities at the single cell level, it is still necessary to run consecutive samples using different red fluorescence threshold values to remove noise and small cells to allow statistically relevant counts of larger cells. In the future, there will certainly be a need to operate with a set of two or three size-class recording protocols or instruments to analyse the complete size spectrum effectively.

ACKNOWLEDGEMENTS

We would like to thank the captain, officers, crew and fellow scientists on board the Royal Research Ship (RRS) Discovery during the D285 cruise. We thank the personnel of the harbour for providing help and facilities for operating the Cytosub.

FUNDING

The temporal study was supported by the CYMIS contract between CNRS and the City of Marseille, partially supported by "l'Agence de l'Eau Rhône Méditerranée Corse". The inter-comparison between NOCS and LMGEM Cytosubs was supported by the ALLIANCE programme, managed by the British Council and the French Foreign Affairs Ministry (MAE).

REFERENCES

Alpine, A. E. and Cloern, J. E. (1988) Phytoplankton growth rates in a light-limited environment, San Fransisco Bay. *Mar. Ecol. Prog Ser.*, **44**, 167–173.

Blanchot, J., Andre, J.-M., Navarette, C. *et al.* (1997) Picophytoplankton dynamics in the equatorial Pacific: diel cycling from flow-cytometer observations. *Comptes Rendus de l'Academie des Sciences - Series III - Sciences de la Vie*, **320**, 925–931.

Brando, B., Göhde, W., Jr, Scarpati, B. *et al.* (2001) The "vanishing counting bead" phenomenon: Effect on absolute CD341 cell counting in phosphate-buffered saline-diluted leukapheresis samples. *Cytometry*, **43**, 154–160.

Burkill, l. P. H. (1987) Analytical flow cytometry and its application to marine microbiology. *Microbes in the sea*. Ellis Horwood limited.

Campell, J. W. and Yentsch, C. M. (1989) Variance within homogeneous phytoplankton populations, I: theoretical framework for interpreting histograms. *Cytometry*, **10**, 587–595.

Cassie, R. M. (1963) Microdistribution of plankton. In Barnes, H. (eds), *Oceanogr. Mar. Biol. Annual rev.*, **1**, 223–252.

Doubell, M. J., Seuront, L., Seymour, J. R. *et al.* (2006) High-resolution fluorometer for mapping micro scale phytoplankton distributions. *AEM*, **72**, 4475–4478.

Dubelaar, G. and Gerritzen, P. (2000) CytoBuoy: a step forward towards using flow cytometry in operational oceanography. *Sci. Mar.*, **64**, 255–265.

Dubelaar, B. J., Gerritzen, P., Beeker, A. E. R. *et al.* (1999) Design and first results of Cytobuoy: a wireless flow cytometer for in situ analysis of marine and fresh waters. *Cytometry*, **37**, 247–254.

Dubelaar, B. J., Venekamp, R. R. and Gerritzen, P. L. (2003) Handsfree counting and classification of living cells and colonies. *6th Congress on Marine Sciences*, Havana.

Falkowski, P. G., Laws, E. A., Barber, R. T. *et al.* (2003) Phytoplankton and their role in Primary, new, and export production. *The role of the Ocean Carbon Cycle in Global Change*. M. J. R.Fasham.

Field, C. B., Behrenfeld, M. J., Randerson, J. T. *et al.* (1998) Primary production of the biosphere: integrating terrestrial and oceanic components. *Science*, **281**, 237–240.

Furnas, M. J. (1991) Net *in situ* growth rates of phytoplankton in an oligotrophic, tropical shelf ecosystem. *Limnol. Ocenaogr.*, **36**, 13–29.

Gosset, W. S. (1907) On the error of counting with a haemocytometer. *Biometrika*, **5**, 351–360.

Guillard, R. R. L. (1975) Culture of phytoplankton for feeding marine invertebrates. *Culture of marine invertebrate animals*. Plenum Press, New York.

Huisman, J., van Oostveen, P. and Weissing, F. J. (1999) Species dynamics in phytoplankton blooms: incomplete mixing and competition for light. *Am. Nat.*, **154**, 46–68.

Hutchinson, G. E. (1961) The Paradox of the Plankton. *Am. Nat.*, **95**, 137–145.

Kirchman, D., Sigda, J., Kapuscinski, R. *et al.* (1982) Statistical analysis of the direct count method for enumerating bacteria. *AEM*, **44**, 376–382.

Kosakowska, J. A. (2002) Pigment composition in relation to phytoplankton community structure and nutrient content in the Baltic Sea. *Oceanologia*, **44**, 419–437.

Li, W. K. W. (1997) Cytometric diversity in marine phytoplankton. *Limnol. Oceanogr.*, **42**, 874–880.

Mahadevan, A. and Campbell, J. W. (2002) Biogeochemical patchiness at the sea surface. *Geophys. Res. Lett.*, **29**, 1–4.

Martin, A. P., Zubkov, M. V., Burkill, P. H. *et al.* (2005) Extreme spatial variability in marine picoplankton and its consequences for interpreting Eulerian time-series. *Biol. Lett.*, **1**, 366–369.

Mitchell, J. G., Yamazaki, H., Seuront, L. *et al.* (2006) Phytoplankton patch patterns: seascape anatomy in turbulent ocean. *J. Mar. Syst.*, DOI:10.1016/j.jmarsys.2006.01.019.

Morris, I. (1980) The physiological ecology of phytoplankton. Blackwell Sci. Publ, Berkley, 625 pp.

Nyquist, H. (1928) Certain topics in telegraph transmission theory. *Trans. AIEE*, **47**, 617–644.

Olson, R. J. and Sosik, H. M. (2007) A submersible imaging-in-flow instrument to analyze nano and microplankton: Imaging FlowCytobot. *Limnol. Oceanogr. Meth.*, **5**, 193–203.

Olson, R. J., Shalapyonok, A. and Sosik, H. M. (2003) An automated flow cytometer for analyzing pico- and nanophytoplankton = FlowCytobot. *Deep-Sea Res. II*, **50**, 301–315.

Platt, T. (1981) Physiological basis of phytoplankton ecology. *Can. J. Fish. Aquat. Sci.*, **210**, 1–346.

Rantajarvi, E., Olsonen, R., Hallfors, S. *et al.* (1998) Effect of sampling frequency on detection of natural variability in phytoplankton: unattended high-frequency measurements on board ferries in the Baltic Sea. *ICES J. Mar. Sci.*, **55**, 697–704.

Sarmiento, J. L. and Bender, M. (1994) Carbon biogeochemistry and climate change. *Photosyn. Res.*, **39**, 209–234.

Shapiro, H. M. (2003) *Practical Flow Cytometry*. John Wiley & Sons, New Jersey.

Sieracki, C. K., Sieracki, M. E. and Yentsch, C. M. (1998) An imaging in flow system for automated analysis of microplankton. *Mar. Ecol. Prog Ser.*, **168**, 285–296.

Smayda, T. J. (1998) Patterns of variability characterizing marine phytoplankton, with examples from Narragansett Bay. *ICES J. Mar. Sci.*, **55**, 562–573.

Sosik, H. M., Olson, R. J., Neubert, M. G. *et al.* (2003) Growth rates of coastal phytoplankton from time-series measurements with a submersible flow cytometer. *Limnol. Ocenaogr.*, **48**, 1756–1765.

Sosik, H. M. and Olson, R. J. (2007) Automated taxonomic classification of phytoplankton sampled with imaging-in-flow cytometry. *Limnol. Oceanogr. Meth.*, **5**, 204–216.

Stewart, W. D. P. (1974) *Algal Physiology and Biochemistry*. Blackwell, Oxford.

Takahashi, T., Olafson, J., Goddard, J. G. *et al.* (1993) Seasonal variation of CO_2 and nutrients in the high-latitude surface oceans: a comparative study. *Global Biogeochem. Cycles*, **7**, 843–878.

Vaulot, D. and Marie, D. (1999) Diel variability of photosynthetic picoplankton in the equatorial Pacific. *J. Geophys. Res.*, **104**, 3297–3310.

Young, W., Roberts, A. and Stuhne, G. (2001) Reproductive pair correlations and clustering of organisms. *Nature*, **412**, 328–330.

Zubkov, M. V. and Burkill, P. H. (2006) Syringe pumped high speed flow cytometry of oceanic phytoplankton. *Cytometry Part A*, **69**, 1010–1019.

Zubkov, M. V., Fuchs, B. M., Tarran, G. A. *et al.* (2002) Mesoscale distribution of dominant bacterioplankton groups in the northern North Sea in early summer. *Aquat. Microbial. Ecol.*, **29**, 135–144.